AGU ADVANCING EARTH AND SPACE SCIENCE

Exploring the Influence of Summer Temperature on Human Mobility During the COVID-19 Pandemic in the San Francisco Bay Area

Amina Ly[1] ID**, Frances V. Davenport[1,2,3]** ID**, and Noah S. Diffenbaugh[1,4]** ID

[1]Department of Earth System Science, Stanford University, Stanford, CA, USA, [2]Department of Atmospheric Science, Colorado State University, Fort Collins, CO, USA, [3]Department of Civil and Environmental Engineering, Colorado State University, Fort Collins, CO, USA, [4]Doerr School of Sustainability, Stanford University, Stanford, CA, USA

Abstract Studies on the relationship between temperature and local, small scale mobility are limited, and sensitive to the region and time period of interest. We contribute to the growing mobility literature through a detailed characterization of the observed temperature-mobility relationship in the San Francisco Bay Area at fine spatial and temporal scale across two summers (2020–2021). We used anonymized cellphone data from SafeGraph's neighborhood patterns data set and gridded temperature data from gridMET, and analyzed the influence of incremental changes in temperature on mobility rate (i.e., visits per capita) using a panel regression with fixed effects. This strategy enabled us to control for spatial and temporal variability across the studied region. Our analysis suggested that all areas exhibited lower mobility rate in response to higher summer temperatures. We then explored how several additional variables altered these results. Extremely hot days resulted in faster mobility declines with increasing temperatures. Weekdays were often more resistant to temperature changes when compared to the weekend. In addition, the rate of decrease in mobility in response to high temperature was significantly greater among the wealthiest census block groups compared with the least wealthy. Further, the least mobile locations experienced significant differences in mobility response compared to the rest of the data set. Given the fundamental differences in the mobility response to temperature across most of our additive variables, our results are relevant for future mobility studies in the region.

Plain Language Summary Studies on the relationship between temperature and local, small scale mobility are limited, and sensitive to the region and time period of interest. We used anonymized cellphone data and gridded daily temperature data to explore how mobility responded to temperature variations in the San Francisco Bay Area during the summer months of 2020 and 2021. Employing a statistical causal inference method that controlled for variability in time and space, we found that almost all areas exhibited decreased mobility in response to higher summer temperatures. However, the rate of decrease was higher on hot days, in wealthier areas, and on weekends. These differences among many groups make our results particularly relevant for mobility studies in highly populated regions, both now and with rising temperatures in the future.

1. Introduction

There exist few studies that measure the influence of temperature variations on local, daily mobility (which we refer to as "mobility" for the remainder of the text) at fine spatial and temporal scales. The existing literature investigating the relationship between mobility and weather has resulted in a range of results (Böcker et al., 2013). Some studies generally assume that mobility increases during warmer seasons (Böcker et al., 2016; Liu et al., 2014; Zacharias et al., 2004). However, the relationship extends beyond the annual cycle, and daily weather patterns–including snow, rain, fog, and storms–can significantly affect mobility (Cools et al., 2010; Creemers et al., 2015). The level of influence that these weather patterns are reported to have varies from study to study. For example, studies in North America and Europe have found conflicting evidence of temperature influence, potentially due to differences in popularity of open-air commutes (e.g., walking and biking) (Pucher & Buehler, 2012). It is likely that much of this disagreement is due to variability in climate and social conditions of the studied area (Böcker et al., 2013), and therefore further investigation into the relationships between mobility and weather are likely to benefit from focusing on a specific region and time period.

In addition to the limited understanding of the current relationship between temperature and mobility, exposure to extreme temperatures is increasing. In the US, incidents of extreme heat have increased in both intensity

and duration since the 1960s (IPCC, 2021). This trend is anticipated to continue into the rest of the century even in aggressive decarbonization scenarios (Collins et al., 2013; Diffenbaugh & Ashfaq, 2010; Diffenbaugh et al., 2018), thereby increasing the exposure of the US population to these events (Batibeniz et al., 2020; IPCC, 2021; Reidmiller et al., 2018).

These historical and projected changes are of particular interest when paired with the fact that addressing any potential heat stress often includes daily mobility. Typically, heat stress is managed using air conditioning, public cooling centers, and public awareness campaigns and warning systems (Bassil et al., 2009; Eisenman et al., 2016; Palecki et al., 2001). Many of the interventions that combat the risks of intensifying heat events include some amount of local travel. This includes traveling to cooling centers and conducting wellness checks on vulnerable individuals who lack air conditioning (Widerynski et al., 2017). Characterizing typical mobility patterns in response to increasing temperatures is thus critical for minimizing health risks associated with extreme heat exposure by anticipating need for wellness services during heatwaves, supporting accessibility efforts, and limiting strain on public health services.

The COVID-19 pandemic resulted in the release of a number of data products on mobility to aid in disease-mitigation efforts. Our study period takes place during the pandemic and provides a unique context through which to interpret our findings. After the declaration of a worldwide pandemic by the World Health Organization in March 2020 (WHO, 2020), numerous countries began to implement travel and mobility restrictions as their main non-pharmaceutical intervention to reduce the number of COVID-19 infections within their borders. By 20th April 2020, 100% of travel destinations had some form of travel restrictions in place, of which 45% partially or completely closed borders to tourists, 18% banned individuals traveling from select countries, and 7% applied quarantine or self-isolation requirements (UNWTO, 2020).

In the US, individual states and counties implemented their own restrictions, with regulations often differing between neighboring municipalities. Twenty-four states established travel restrictions that included periods of isolation and testing requirements for those entering the state (Studdert et al., 2020). Government responses were highly variable in space and time as individual states and municipalities instituted their own guidelines and ordinances in the absence of blanket federal orders (Diffenbaugh et al., 2020). COVID-19 shelter in place protocols did change mobility patterns across the country, and many regions saw an increase in the frequency of visitations to public, outdoor spaces (Wu et al., 2021). California specifically implemented travel guidance and allowed counties to impose additional restrictions as they saw fit (Aragón, 2021). Workplace and school closures were calculated to be effective measures in avoiding COVID-19 deaths in the San Francisco (SF) Bay Area (Head et al., 2020). As a result of this guidance and quantitative models supporting the efficacy of closures, schools and "non-essential" businesses were closed and shifted to a virtual environment.

The SF Bay Area was one of the early epicenters of COVID-19 transmission in the US, and since then had consistently maintained some of the country's most restrictive pandemic management policies (Studdert et al., 2020). Beginning with a multi-county stay-at-home order in March 2020, these shelter in place policies heavily restricted business operations and travel for the subsequent year. In addition, the SF Bay Area has the second lowest rates of at-home cooling among major metropolitan areas in the US, with only 47% of households reporting at-home air conditioning in 2019 (American Housing Survey, 2018; Jung, 2021). This means that most households rely on cooling methods other than domestic air-conditioning during periods of extreme heat. Further, the region exhibits a classic summer-dry "Mediterranean" climate (Ekstrom & Moser, 2012; Hobbs et al., 1995), enabling investigation of the temperature-mobility relationship in the absence of the potentially confounding effect of precipitation variability during the hot season. For these reasons, the summer season in the SF Bay Area region is an ideal testbed to further investigate the relationship between temperature and local, daily mobility in the context of the pandemic.

Several studies have identified that differences in socio-economic status (O'Neill et al., 2005; Vant-Hull et al., 2018) and the built environment (Eisenman et al., 2016; Gronlund & Berrocal., 2020) are associated with varied vulnerability to heat exposure throughout the US. This heterogeneity in socio-demographics points to the value of considering how these spatially defined characteristics may result in varied mobility responses to both socio-political and climatic conditions. To that end, we used data from personal mobile devices to characterize the small-scale, daily movement patterns across the SF Bay area throughout the pandemic period of 2020–2021. We then used panel regressions with fixed effects to characterize the relationship between temperature and mobility

during the summer months. We finally explored the influence of period of the week, extreme heat, income, and how the most and least mobile locations responded to temperatures during this study period.

2. Materials and Methods

2.1. Data

2.1.1. gridMET Temperature Product

We utilized the gridMET 4-km gridded daily maximum temperature data (Abatzoglou, 2013) to calculate temperature in the SF Bay Area region. The gridMET data set uses climatically aided interpolation to derive a product combining Parameter-elevated Regressions on Independent Slopes Model gridded climate data and North American Land Data Assimilation System - 2 regional reanalysis. To quantify the impact of high temperatures on mobility, we selected all data from May to September. See Section 2.2 "Selection of analysis period."

2.1.2. US Census

Using the 2020 census block group boundaries from the US Census, we calculated the mean daily high temperature of all gridMET grid cells that fall within a given block group. We did this by extracting the gridMET raster values within a US census block group polygon using the exactextractR library in R (Baston, 2022). This was used to obtain a time series of the high temperature by block group each day from 1979 to 2021. We assigned a population weighted income group to each block group using the 2019 US Census Bureau's American Community Survey's (ACS) 5-year estimates of population and median income (US Census Bureau, 2022). See Section 2.3 "Census block group analysis."

2.1.3. SafeGraph Mobility Data

We analyzed local, daily mobility patterns using the SafeGraph Neighborhood Patterns data set (SafeGraph, 2022). The SafeGraph data set is created by analyzing anonymized pings from mobile devices and contains footfall data for each block group from January 2018 to the present day. For this analysis we only utilized data starting in 2020 due to notes from SafeGraph on methodology changes in early 2020 (SafeGraph, 2022). This change prevents the comparison of data from 2018 to 2019 and any succeeding years. In the SafeGraph data, any devices that are recorded in a block group for less than a minute are removed, and the remaining devices are counted as a "stop." Each stop data point includes information on the date, hour, and block group of the recorded stop. Due to data constraints associated with SafeGraph's privacy policy (SafeGraph, 2022), the source information includes only the number of devices that spent time in the block group and not information about whether a stop was made by a home device or a non-resident device. An accompanying SafeGraph data set contains a monthly estimate of the total number of home devices based on devices' nighttime activity. SafeGraph adds Laplacian noise as a differential privacy technique to protect individual privacy, which adds slight, random noise to device estimates. Although SafeGraph does not receive demographic data from their providers due to privacy concerns, they have affirmed independently that the data are well-sampled among different demographics as noted in their documentation (SafeGraph, 2022).

2.1.4. Air Quality Data

Wildfires in the Bay Area during the summer and autumn of 2020 and 2021 caused several poor air quality days where residents were instructed to limit travel and remain indoors (Bay Area Air Quality Management District's (BAAQMD), 2021). In order to exclude the influence of days where this additional public intervention was introduced, we removed data points from all data sets for the 12 days where at least one county in the SF Bay Area recorded a BAAQMD Air Quality Index value of ≥151 (for which the BAAQMD recommends all individuals should limit prolonged outdoor exertion).

2.2. Selection of Analysis Period

Unless stated otherwise, all analyses were completed for data points falling between May and September in 2020 and 2021. As described above, we restricted our analysis to dates after 2020 due to inconsistencies in the SafeGraph data. We also focused on dates between May and September, which we refer to as "summer" for the remainder of the text. These summer months were selected since at least some block groups experienced temperatures at or above their historic 95th percentile during this time. In addition, the region typically experiences dry

summers, and this allowed us to avoid introducing precipitation as a confounding variable. Rainfall in the region for summer 2020 and 2021 was limited (Figure S1 in Supporting Information S1), and we further confirmed that the inclusion of the minimal precipitation does not add value to our models (Table S1, Text S1, and Figure S5 in Supporting Information S1). Finally, these months align relatively well with early pandemic closures in 2020, and reopenings in 2021 (Eby, 2023). While we do not draw any direct causal relationships between mobility and pandemic-related social environments, closures, and non-pharmaceutical interventions in this study, the pandemic offers valuable context through which the results may be interpreted, as further explored in our Section 4.

2.3. Creation and Interpretation of Mobility Index

Using the SafeGraph data set, we created a mobility index (MI) that allowed us to compare mobility across block groups, and thereby characterize movement across the SF Bay Area. This MI was designed to address some of the limitations of the SafeGraph data set, such as the ambiguity between stops by visitors and stops by home devices. To address this limitation, we estimated the daily number of visits as the number of total stops minus home devices in that block group (i.e., we removed the devices identified by SafeGraph as "home devices," the remaining number of devices estimated to be either "visitors" to the location or a home device that left and returned that day). We then divided the number of visits by the number of home devices in each block group to normalize the value and calculate our final daily MI value.

Because we normalize by the number of home devices, MI should be interpreted as a measure of visitation rate for any given block group on a given day, including both those visiting from alternate locations and those residents of a block group who may leave and return within a 24-hr period. This allows for a general interpretation of how "busy" a location might be compared to the alternative where there is no measured movement into a location. When MI is equal to zero, it is estimated that no outside devices entered the location, and no home devices left and returned that same day. When it is below zero, the number of recorded devices is fewer than the estimate of home devices made by SafeGraph. This is an artifact of the random Laplacian noise added by SafeGraph, and should not impact overall analysis (SafeGraph, 2022).

2.4. Census Block Group Analysis

To further understand how demographics may influence the relationship between a block group and mobility during the hottest part of the year, we used American Community Survey's 5-year estimates of population and median income by block group (US Census Bureau, 2022). We assigned each block group to an income group between 1 ("Low" income) and 5 ("High" income). We weighted this grouping by population, so that the Low income group represented the lowest earning 20% of the population in the SF Bay Area, the Medium Low income group the lowest 20%–40% of earners, and so on. This weighting ensured that there were roughly the same number of individuals represented in each income group. We also assigned each block group to an MI group, with the least mobile block groups (<5th percentile) labeled as the "Low" MI group, block groups from the 5th–95th percentile labeled as "Intermediate" groups, and the most mobile block groups (>95th percentile) labeled as the "High" MI group.

We plotted the distribution of the MI for each income group. In addition, we tested whether the distributions were different between income groups by comparing all pairings of income groups using two non-parametric tests: a two-sample Kolmogorov-Smirnov (K-S) test, and a Wilcoxon Rank Sum Test. The K-S test is sensitive to differences in both location and shape of the distributions, and the null hypothesis is that the two samples are drawn from the same underlying distribution. The Wilcoxon test's null hypothesis is that the two distributions are the same and have the same median.

2.5. Panel Regression With Fixed Effects

We completed several analyses using panel regressions with fixed effects. This is a causal inference technique that enabled us to establish a relationship between mobility and daily maximum temperature. This method was particularly valuable because it allowed us to control for invariant differences between block groups, subtract out average differences in mobility between them, and account for any differences in shelter in place orders between the different sub-regions of the SF Bay Area. The time fixed effects variable subtracted out month-to-month,

week-of-year, and annual mobility variations (when applicable)—accounting for seasonal changes, as well as shifts in mobility due to week-to-week variation driven by holidays and short-term shocks, and annual differences between 2020 and 2021. When compared to using a daily time fixed effects variable, the week, month, and year fixed effect led to a smaller 95% confidence interval (Figure S2 in Supporting Information S1). With these controls, this model allowed us to isolate the effect of temperature on mobility from spatial and temporal confounding factors.

We used the daily high temperature at the block group level as the independent variable, and the daily MI at the block group level as the dependent variable. For this analysis, we transformed the MI by taking the cube root of MI values. To do so, we took the cube root of the absolute value of each MI, and multiplied the result by the sign of the original MI. Unlike a log transformation, this strategy allows us to maintain zeros and negative MI values while addressing the skewed MI values (Figure S3 in Supporting Information S1). In addition, we completed supplementary calculations with log-transformed MI values (where 1.0001 was added to each MI value) and compared those results to the cube-root-transformed data set (Figure S2 in Supporting Information S1).

We estimated the 95% confidence intervals of each model using a bootstrap resampling technique clustered by county. We resampled the original data by county with replacement to obtain a new data set of the same length as the original data set and re-ran the same regression on the new subset. We repeated this process 1,000 times to obtain a range of model outputs. Of the resulting model coefficients, we used the 2.5 and 97.5th percentile coefficient values as the minimum and maximum values for our 95% confidence interval range.

2.5.1. MI Response to Temperature

Our first two linear panel regressions with fixed effects tested the response of $\sqrt[3]{\text{MI}}$ to temperature changes using our summer data set. In addition, we also calculated the panel regression using a subset of the data that only included days where at least 5% of block groups experience temperatures at or above their historic 95th percentile (which we refer to as "hot days." See Text S2, Figure S6 in Supporting Information S1 for details):

$$\sqrt[3]{(Y_{ct})} = \beta X_{ct} + n_c + \delta_t + \varepsilon_{ct} \tag{1a}$$

where Y_{ct} is the expected MI value in block group c on a given day t; β is the estimated coefficient; X is the average daily maximum high temperature of block group c on day t; n_c is the block group fixed effect; δ_t is the year, month, and week-of-year fixed effect created by concatenating the year, month, and number of complete 7 day periods that have occurred between the date and 1st January of the year; and ε_{ct} is an error term.

We also calculated the relationship between temperature and MI for each year. As before, we did this for the full summer and for a data set that only included hot days. The data were separated into two subgroups based on the year. We then used a similar equation that did not include a year fixed effect:

$$\sqrt[3]{(Y_{ct})} = \beta X_{ct} + n_c + \gamma_t + \varepsilon_{ct} \tag{1b}$$

where Y_{ct} is the expected MI value in block group c on a given day t; β is the estimated coefficient; X is the average daily maximum high temperature of block group c on day t; n_c is the block group fixed effect; γ_t is the month, and week of year fixed effect; ε_{ct} is an error term. This first panel regression analysis pooled all income groups.

2.5.2. Interaction Variables

We followed this analysis with further investigation into several variables that had the potential to influence mobility. These analyses added an interaction term that assigned each data point with either Equations 2a and 2b: weekday or weekend, Equations 3a and 3b: the population weighted income group, or Equations 4a and 4b: mobility group. This structure allowed us to compare the relationship between MI and temperature with many influences. First, we considered the difference in response for weekend and weekdays:

$$\sqrt[3]{(Y_{ct})} = \beta X_{ct} W_g + n_c + \delta_t + \varepsilon_{ct} \tag{2a}$$

where Y_{ct} is the expected MI value in block group c on a given day t; β is the estimated coefficient; X is the average daily maximum high temperature of block group c on day t; W_g is one of either "Weekend" (Saturday and Sunday) or "Weekday" (all other days); n_c is the block group fixed effect; δ_t is the month, week of year, and year fixed effect; ε_{ct} is an error term.

We calculated the above relationships with annual subgroups that did not include a year fixed effect:

$$\sqrt[3]{(Y_{ct})} = \beta X_{ct} W_g + n_c + \gamma_t + \varepsilon_{ct} \tag{2b}$$

where Y_{ct} is the expected MI value in block group c on a given day t; β is the estimated coefficient; X is the average daily maximum high temperature of block group c on day t; W_g is one of either "Weekend" (Saturday and Sunday) or "Weekday" (all other days); n_c is the block group fixed effect; γ_t is the month, and week of year fixed effect; ε_{ct} is an error term.

We then modeled the influence of wealth on the relationship between temperature and MI by assigning a population-weighted income group to each data point and used that value as an interaction term. We utilized median income as a proxy for other factors that may influence mobility and are correlated with income at the block group (Downey, 1998; Reid et al., 2009). These include socio-economic status, population density, infrastructure, and land use type. We characterized the relationship between temperature and mobility across five income groups using a cube root specification:

$$\sqrt[3]{(Y_{ct})} = \beta X_{ct} I_c + n_c + \delta_t + \varepsilon_{ct} \tag{3a}$$

where Y_{ct} is the expected MI value in block group c on a given day t; β is the estimated coefficient; X is the average daily maximum high temperature of block group c on day t; I_c is the block group's assigned population-weighted income group; n_c is the block group fixed effect; δ_t is the month, week of year, and year fixed effect; ε_{ct} is an error term.

Then we completed a similar calculation with annual subgroups without the year fixed effect:

$$\sqrt[3]{(Y_{ct})} = \beta X_{ct} I_c + n_c + \gamma_t + \varepsilon_{ct} \tag{3b}$$

where Y_{ct} is the expected MI value in block group c on a given day t; β is the estimated coefficient; X is the average daily maximum high temperature of block group c on day t; I_c is the block group's assigned population-weighted income group; n_c is the block group fixed effect; γ_t is the month, and week of year fixed effect; ε_{ct} is an error term.

There was significant skew in the mobility data (Figure S3 in Supporting Information S1), prompting further investigation into the block groups with uncommon mobility patterns at the extreme tails of the distribution. We selected thresholds that separate block groups that exhibited extremely low or high mobility compared to the rest of the data set. From there we calculated the influence of temperature on MI for the block groups that were on the high and low extremes of average summer MI, and compared it to the rest of the data set. We assigned each block group a percentile MI value compared to the rest of the SF Bay Area. Any block groups in the bottom 5% were assigned the "Low" MI group, those in the top 5% were assigned the "High" MI group, and the rest were marked as "Intermediate" MI. We characterized the relationship between temperature and mobility across the MI groups, again using a cube root specification:

$$\sqrt[3]{(Y_{ct})} = \beta X_{ct} M_c + n_c + \delta_t + \varepsilon_{ct} \tag{4a}$$

where Y_{ct} is the expected MI value in block group c on a given day t; β is the estimated coefficient; X is the average daily maximum high temperature of block group c on day t; M_c is the block group's assigned MI group; n_c is the block group fixed effect; δ_t is the month, week of year, and year fixed effect; ε_{ct} is an error term.

We performed a similar calculation with annual subgroups without the year fixed effect:

$$\sqrt[3]{(Y_{ct})} = \beta X_{ct} M_c + n_c + \gamma_t + \varepsilon_{ct} \tag{4b}$$

where Y_{ct} is the expected MI value in block group c on a given day t; β is the estimated coefficient; X is the average daily maximum high temperature of block group c on day t; M_c is the block group's assigned MI group; n_c is the block group fixed effect; γ_t is the month, and week of year fixed effect; ε_{ct} is an error term.
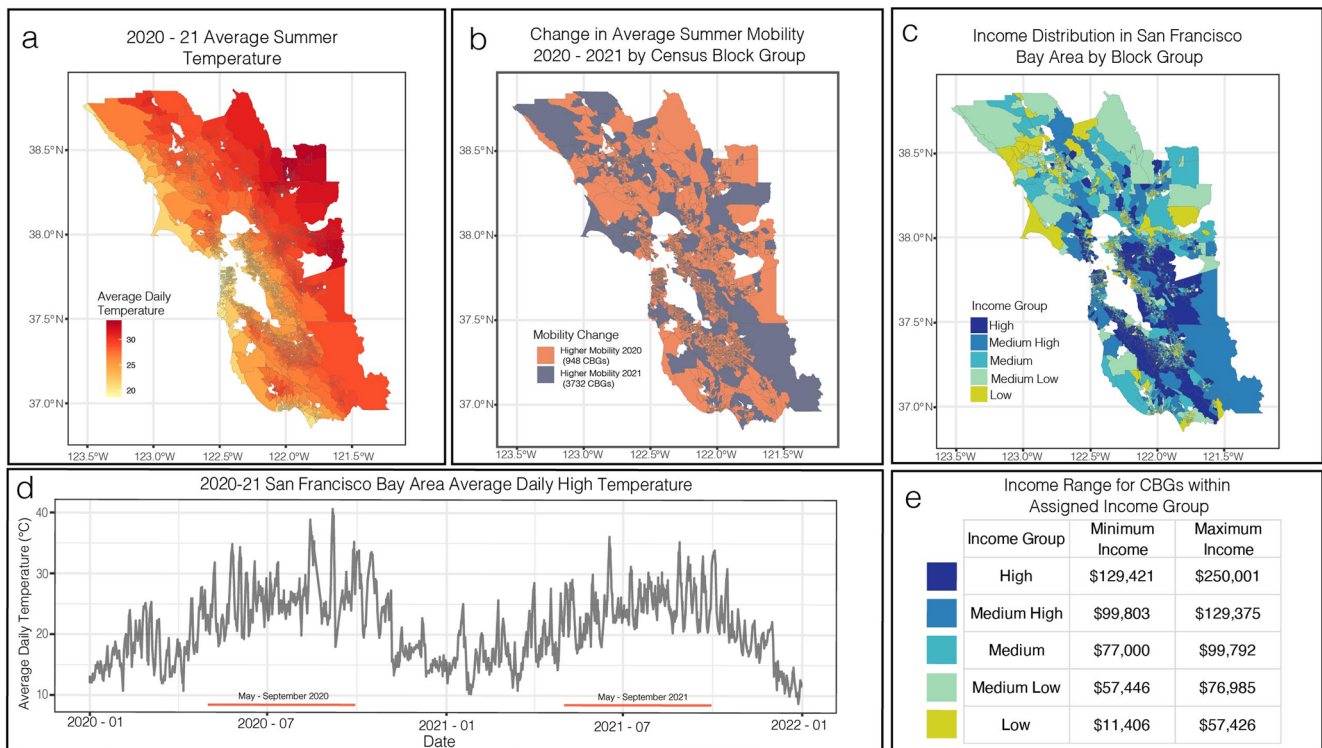
Figure 1. Overview of data included in analysis. (a) Daily high temperature was calculated by averaging the maximum daily temperature of all gridMET grid cells within a census block group (block group) each day. (b) Mobility index change was calculated as the sign of the difference between 2020 and 2021. Block groups with a higher value in 2020 are shown in orange; block groups with a higher value in 2021 are shown in purple. (c) Each block group was assigned an income group between 1 (Low income) and 5 (High income). Income groups were weighted by population (see Section 2). (d) Region-wide average daily temperature in 2020 and 2021 for the San Francisco Bay Area. (e) A table with the maximum and minimum income of each assigned income group. Average summer temperature (a) and mobility (c) only reflect data for days between May and September, which are delineated in red along the *x*-axis in (d). Temperature recordings from 28 October 2021 to 31 October 2021, were removed from the gridMET data set due to suspected record error. Panel regression analysis did not include data in this month, and therefore did not affect results of the analysis.

3. Results

3.1. General Data Set Patterns

As expected, during the summer of 2020 and 2021, areas closer to the ocean tended to experience cooler temperatures (~20°C), while those further inland experienced much higher average summer temperatures (~30°C) (Figure 1a). Likewise, inland block groups had more days with temperatures at or above the 95th percentile (~34°C), as opposed to block groups closer to the coast or San Francisco Bay (Figure S4a in Supporting Information S1). The average MI in all of 2020 and 2021 was 1.20 (median = 0.69), and 1.24 (median = 0.71) in the summer. In 2020, our calculated MI was generally lower on hot days (mean = 0.86, median = 0.50) than in 2021 (mean = 1.60, median = 0.96) (Figure 1b). Of the 4,722 CBGs included in the calculation, 3,766 (80%) increased in mobility from 2020 to 2021. Of those 3,766, 3,026 (80.3%) experienced at least a 50% increase in mobility.

We assigned block groups different income groups by population to investigate the variable responses to MI by income (Figure 1e). Each group represented 20% of the population of the SF Bay Area. As reported by the ACS, the median annual income of block groups in the SF Bay Area ranged from $11,406 to $250,001, with the average value across all block groups in the SF Bay Area being ~$95,774 (median = $88,000) (Figures 1c and 1e). For comparison, the national average income for the US was ~$68,461 (median = $60,000).

Our MI estimated the number of visits to a block group, normalized by the number of residents. The largest decrease in MI took place from mid-March to early-April of 2020–coinciding with the shelter in place policies that first began on 17 March 2020, in SF Bay Area counties (San Francisco Department of Health (SFDoH), 2020). The mean MI during the first 30 days of shelter in place policies was 0.15, with the lowest recorded MI value of −0.47 on 31st March 2020. By definition, a negative MI value indicates fewer devices entering the block
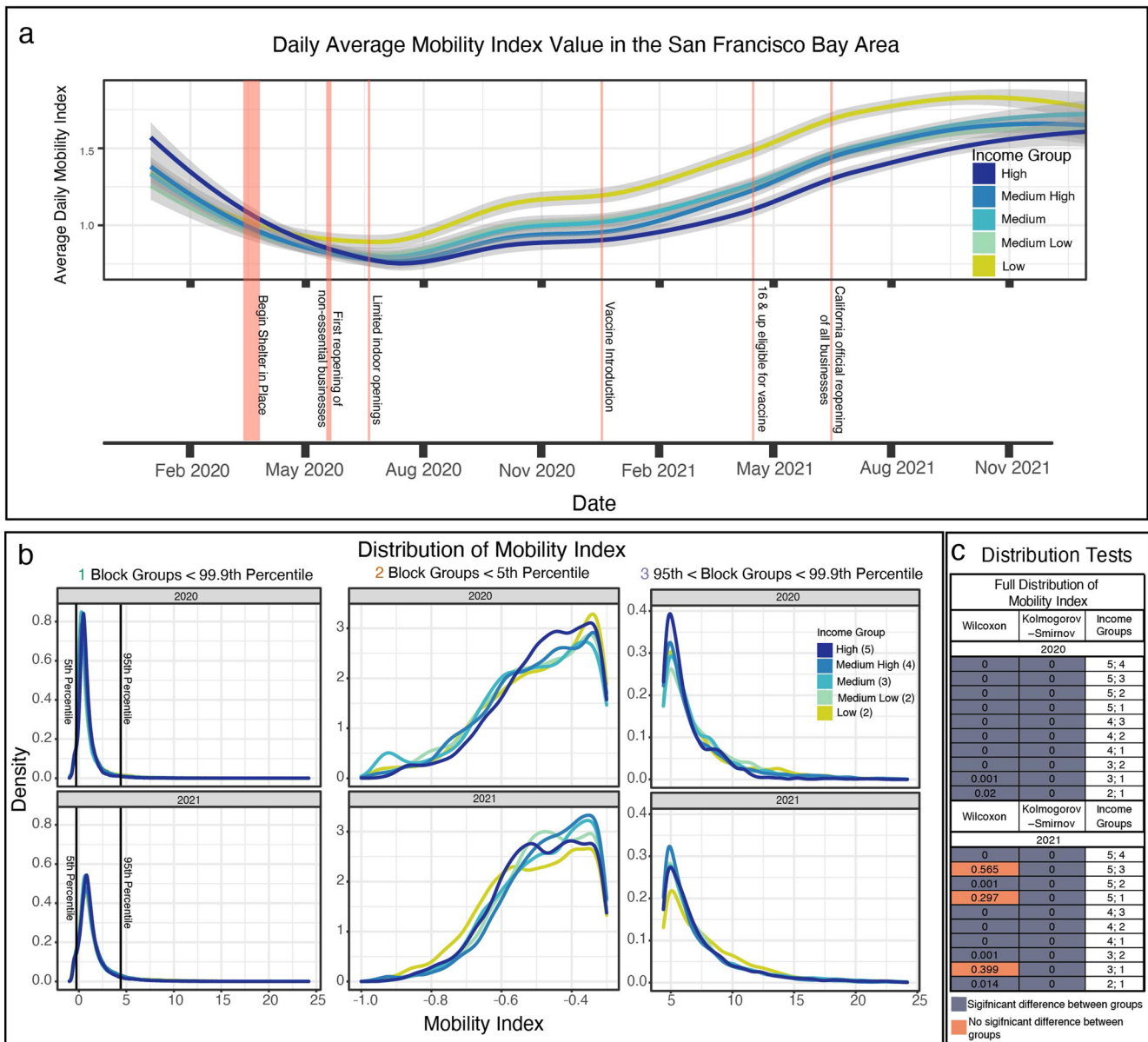
Figure 2. (a) Loess regression of all calculated Mobility Index (MI) values from January 2020 through December 2021, by income group. The shaded area represents the 95% confidence interval of the loess regression. The first shelter in place policies began on 17th March 2020. The red vertical lines are a non-exhaustive list of COVID-19 policy milestones for the reader's reference. (b) Density distribution displayed included values up to the 99.9th percentile (MI = 24.2). (c) All pairings of income groups were compared using a two-sample Kolmogorov-Smirnov (K-S) test, and a Wilcoxon Rank Sum Test. Tests where the *p*-value was ≤0.05 were considered significant are highlighted in purple; tests where the *p*-value was >0.05 are highlighted in orange.

group—including returning home devices—than the number of recorded home devices, and the minimum possible value is −1.0. The average MI in all of 2020 and 2021 was 1.20 (median = 0.69), and 1.24 (median = 0.71) in the summer. Of the 4,722 block groups included in the calculation, 3,766 (80%) increased in mobility from 2020 to 2021. Of those 3,766, 3,026 (80.3%) experienced at least a 50% increase in mobility.

In the first few months of 2020, prior to the start of shelter in place policies, the average MI values were similar among most income groups (Figure 2a). The 95% confidence interval of the loess regression was indistinguishable for block groups with a median household income below $130,000/year (comprising the Low to Medium High income groups). However, there was a noticeable shift in relative MI by all income groups as the start of the COVID pandemic led to implementation of shelter in place policies and closures of many public spaces. The mean MI value changed for all block groups over the course of the 2-year study period, increasing from

their lowest points in early summer 2020. This coincided with the first adjustments to blanket stay at home orders across the SF Bay Area from 18th to 20th May 2020, and the beginning of reopening phases across the state of California on 19th June 2020 (Eby, 2023). MI continued to increase steadily throughout 2021, following the introduction of the first COVID-19 vaccine in late 2020 and its increasing availability throughout 2021 (Eby, 2023). For the summer study period, we compared the MI distribution of each income group and confirmed that the distribution of summer MI was different between the income groups (Figures 2b and 2c). The results were statistically significant for all pairings using the K-S test, and nearly all pairings using the Wilcoxon test; the only exceptions were in 2021 between the High and Medium income groups, High and Low income groups, and Medium and Low income groups in 2021 (Figure 2c).

3.2. Temperature and Mobility Relationship

For all reported panel regression results, unless otherwise stated, all coefficient values (β) were rounded to 4 decimal points, and the *p*-value for any result was <0.001. We first analyzed the relationship between temperature and mobility using a linear regression with fixed effects (Figure 3). The calculated coefficient for the response of MI to variations in temperature was −0.0024. Hence, for every 10°C increase in temperature, the $\sqrt[3]{MI}$ was expected to decrease by ∼0.024 (Figure 3a). To aid in interpretation, we repeated this analysis using a log-transform of MI rather than $\sqrt[3]{MI}$, which yielded a similar prediction of $\beta = -0.0020$. Log-transformed values are often interpreted as the approximate percent change in the original value, therefore this translated to a ∼2% decrease in MI for every 10°C increase in temperature during the summer (Figure S2 in Supporting Information S1). When we refer to the $\sqrt[3]{MI}$ response this change in *Y* is the expected change in the cube root of the mobility rate for any given census block group as temperature diverges from 25°C, and—due to the similarity between the log and cube root transformations—an *approximate* percent change in the mobility rate per degree increase within ∼0.05% of the log-transformed value on average. We provide a table of all our model coefficients with both a cube root and log transformation for reference (Table S2 in Supporting Information S1), a table of all 95% confidence intervals calculated with bootstrap resampling (Table S3 in Supporting Information S1), and an example table of the expected total change in visitors for a location with a median number of residing devices and stops for every 10°C over 25°C (Table S4 in Supporting Information S1).

When we modeled each year independently, we found that while the sign of the response variables remained the same, the rate of decrease shifted from year to year. For each reported β value, the *p*-value was <0.001. During the summer, the $\sqrt[3]{MI}$ decreased faster in 2020 than in 2021 ($\beta_{2020} = -0.0015$, $\beta_{2021} = -0.0011$ in 2021) (Figure 3b). The same analysis on just hot days resulted in $\beta_{hotdays} = -0.0062$, indicating that $\sqrt[3]{MI}$ decreased ∼2.6 times faster (and therefore the mobility rate MI about 17 times faster) per degree increase on hot days compared to the full season (Figure 3c). Hot days resulted in steeper mobility decreases in 2021 compared to 2020 ($\beta_{hotdays, 2020} = -0.0019$, $\beta_{hotdays, 2021} = -0.0037$) (Figure 3d). Notably, estimates that modeled years separately resulted in more conservative estimates and higher r^2 values, indicating a better model fit (Figure 3). There is likely some amount of annual variability that cannot be captured solely through annual fixed effects.

We next considered the potential difference in mobility response on weekends and weekdays by using an interaction variable. Each of the following β values had a *p*-value < 0.001. On weekends, $\sqrt[3]{MI}$ decreased 1.5 times faster—and MI decreased 3.2 times faster—in response to increases in temperature, compared with weekdays ($\beta_{weekend} = -0.0031$; $\beta_{weekday} = -0.0021$) (Figure 4a). When comparing between the 2 years, weekday responses were not substantially different from each other ($\beta_{weekday, 2020} = -0.0008$; $\beta_{weekday, 2021} = -0.0010$), but weekend $\sqrt[3]{MI}$ decreases were about 1.6 times greater—and MI 4.4 times greater—in 2020 than 2021 ($\beta_{weekend, 2020} = -0.0023$; $\beta_{weekend, 2021} = -0.0014$) (Figure 4b). When we further restricted the data set to only model hot days, there was no difference in the response on weekends compared to weekdays ($\beta_{weekend} = -0.0062$; $\beta_{weekday} = -0.0062$) (Figure 4c). When modeling years separately, mobility was reduced at a slower rate in 2020 ($\beta_{weekend, 2020} = -0.0019$; $\beta_{weekday, 2020} = -0.0012$) compared to 2021 ($\beta_{weekend, 2021} = -0.0029$; $\beta_{weekday, 2021} = -0.0035$) (Figure 4d).

To explore how socio-economic differences may have influenced the relationship between mobility and temperature, we added a median-income interaction term to the panel regression model (Figure 5). The coefficients for all income groups were negative which implied decreased mobility in response to higher temperatures ($\beta_{low} = -0.0020$, $\beta_{medium low} = -0.0025$, $\beta_{medium} = -0.0022$, $\beta_{medium high} = -0.0024$, $\beta_{high} = -0.0031$), all with reported *p*-values < 0.001. There was substantial overlap in the confidence intervals for the three intermediate
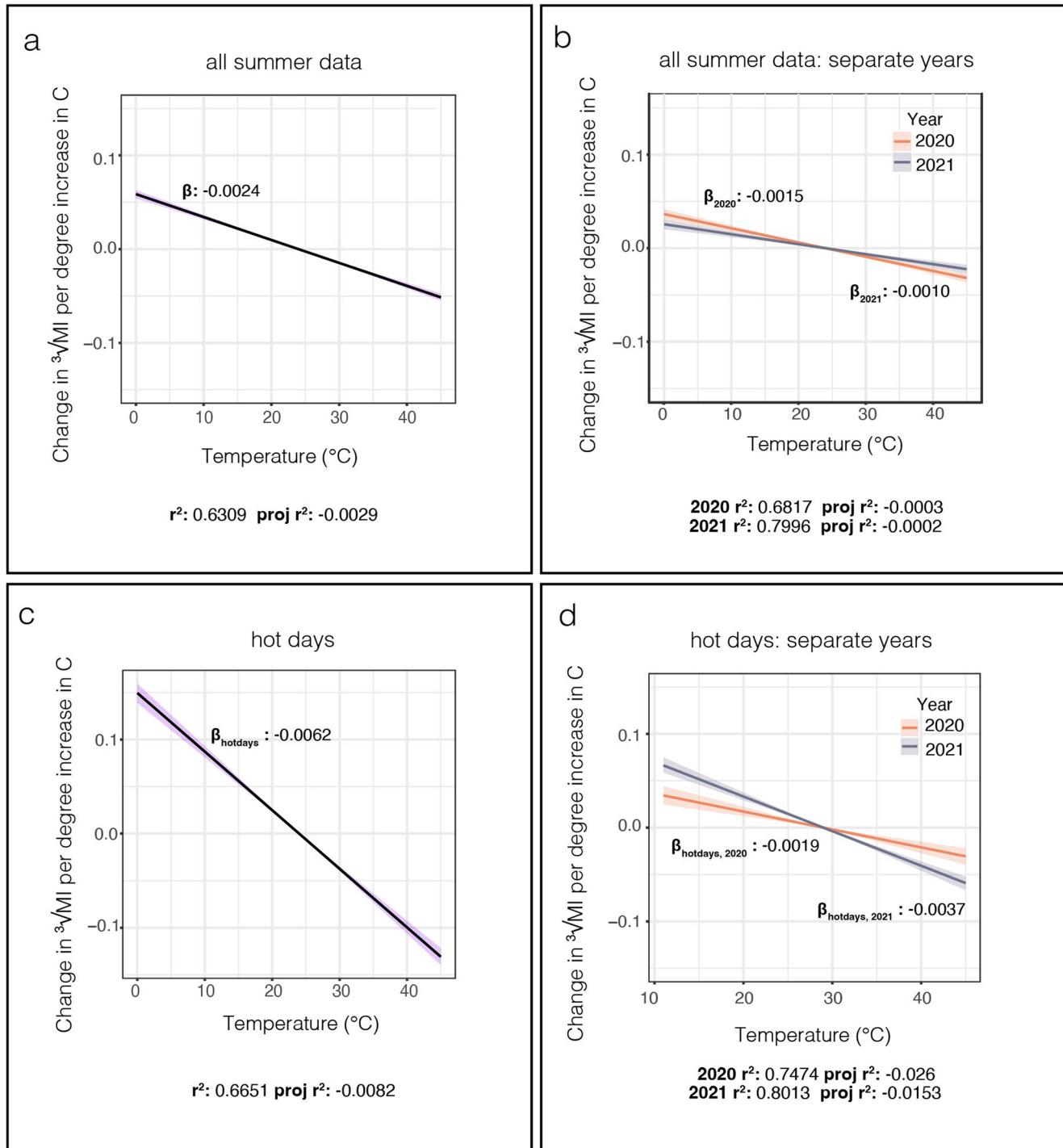
Figure 3. Effect of temperature on mobility index (MI) using fixed effects regression models. Shading of all models indicates 95% CI estimated by bootstrapping by county with replacement (see Section 2). Response functions are all centered at the approximate mean summer temperature for 2020–2021 (25°C). (a) Relationship between temperature and $\sqrt[3]{MI}$ across the San Francisco Bay Area. Median regression model shown with solid purple line. (b) Relationship between temperature and mobility with each year modeled separately, 2020 shown in orange, and 2021 in purple. (c) Relationship between temperature and $\sqrt[3]{MI}$ on data that only includes days where at least 5% of all block groups experienced temperatures above their historic 95th percentile (See Section 2). R^2 and projected (proj) r^2 values are reported for each model. Proj r^2 refers to the r^2 value of the estimated model without including fixed effects.

Change in $\sqrt[3]{}$Mobility Index (MI) with Temperature Interacted with Weekend/Weekday: All Summer Data
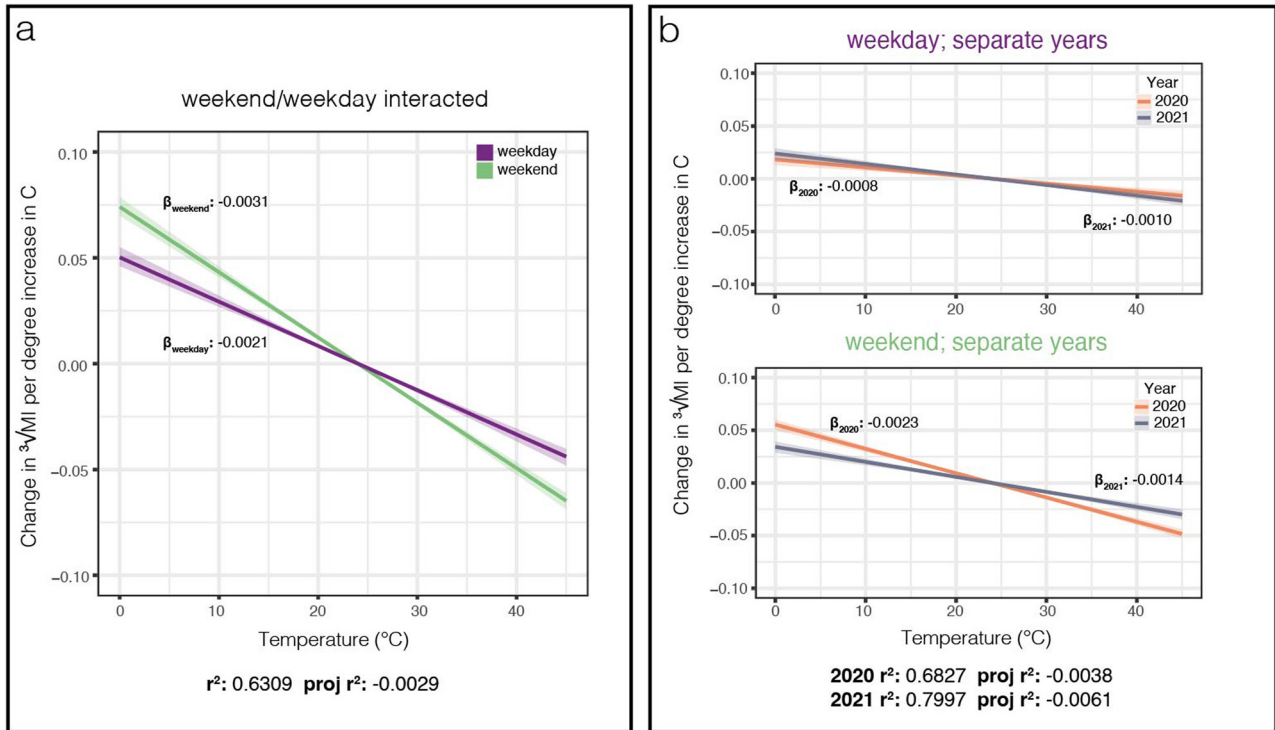
Change in $\sqrt[3]{}$Mobility Index (MI) with Temperature Interacted with Weekend/Weekday: Hot Days Only

Figure 4.

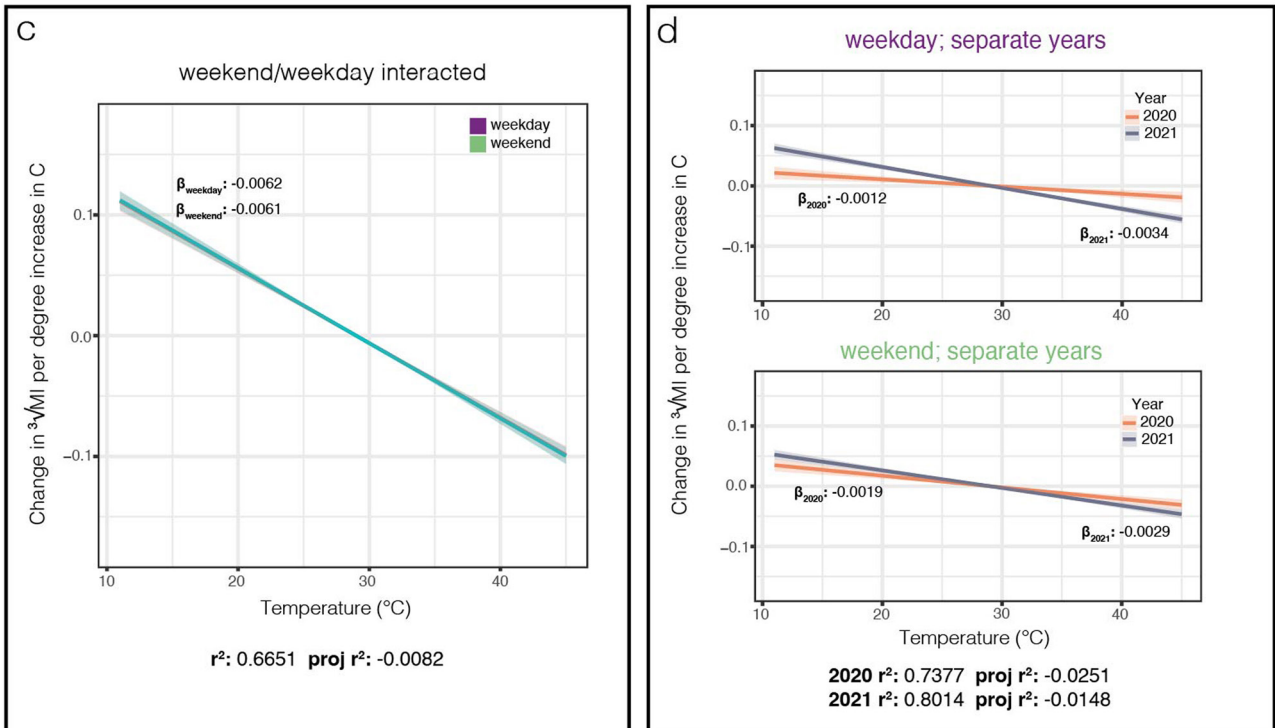Change in $\sqrt[3]{}$Mobility Index (MI) with Temperature:
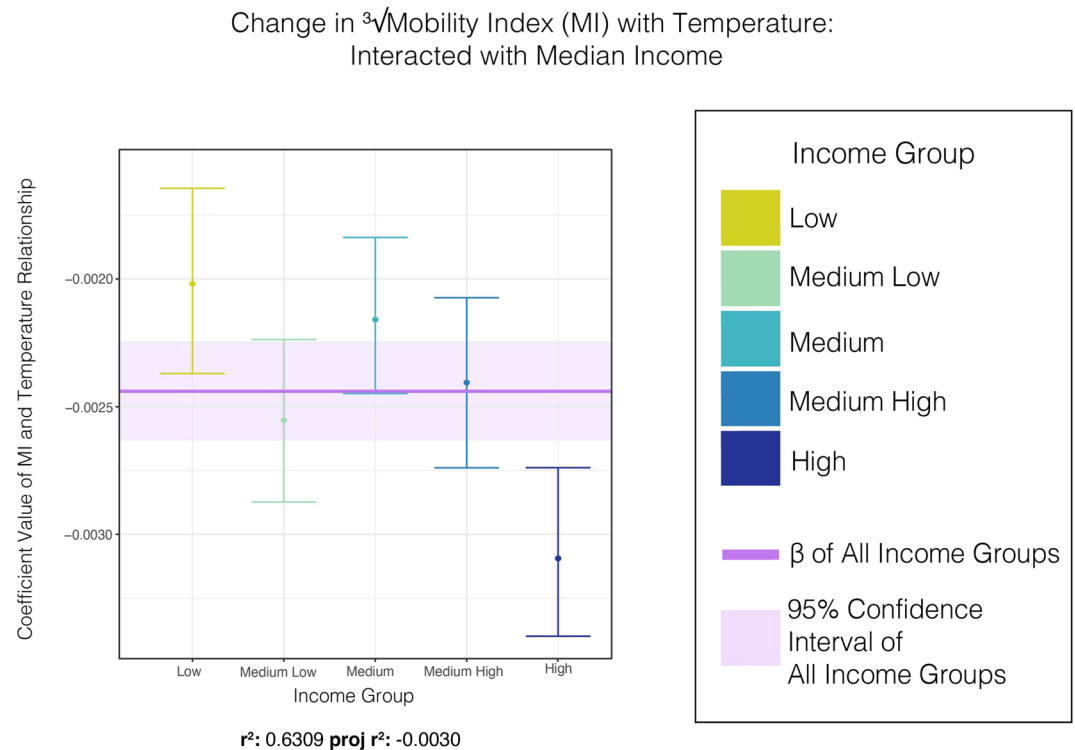Interacted with Median Income

Figure 5. Resulting relationship between mobility index and temperature after the income group interaction variable is integrated into the model. Points show median coefficient estimates and vertical bars show the 95% CI around each point estimate. Solid purple line and shaded area are model results from models in Figure 3a for comparison.

income groups (Medium Low, Medium, and Medium High); however, the confidence intervals for the highest and lowest income groups were entirely distinct from each other. Further, the confidence interval for the High income group was significantly different from even the confidence interval for the pooled fixed effect model that did not distinguish between income groups, with MI in the high income group decreasing 2.2 times faster than the model including all block groups, and 3.72 times faster than the lowest income group.

Finally, we modeled the top and bottom 5% of block groups based on their average summer mobility to see how areas with typically high or low mobility responded to changes in temperature (Figure 6). All presented β values reported p-values < 0.001. When modeled together, the least visited block groups (Low MI) exhibited an increase in mobility with increasing temperatures, in contrast to most of the results from this study ($\beta_{\text{bottom}} = 0.0074$). The most mobile block groups (High MI) decreased $\sqrt[3]{}$MI at a slightly lower rate than block groups from 5th–95th percentile (Intermediate MI) ($\beta_{\text{high MI}} = -0.0023$, $\beta_{\text{intermediate MI}} = -0.0030$). When split between the 2 years, there was again a distinct pattern (Figure 6b): in 2020, the least mobile block groups increased mobility ($\beta_{\text{low MI, 2020}} = 0.0014$), and the most mobile block groups decreased at a rate close to that of our prior analyses ($\beta_{\text{high MI, 2020}} = -0.0010$). In 2021, there was a reversal and the least mobile block groups reduced $\sqrt[3]{}$MI at a much faster rate than the rest of the locations studied ($\beta_{\text{low MI, 2021}} = -0.0075$), and the most mobile block groups increased $\sqrt[3]{}$MI in response to increasing temperatures ($\beta_{\text{high MI, 2021}} = 0.0011$). In both years, block groups in the 5th–95th percentile maintained the negative response in $\sqrt[3]{}$MI, with a slightly faster decline in 2020 than 2021 ($\beta_{\text{intermediate MI, 2020}} = -0.0017$, $\beta_{\text{intermediate MI, 2021}} = -0.0008$). The more conservative estimates made by the analysis

Figure 4. Effect of period of the week on mobility index (MI) using fixed effects regression models. Shading of all models indicates 95% CI estimated by bootstrapping by county with replacement (see Section 2). Response functions are all centered at the approximate mean summer temperature for 2020–2021 (25°C). (a) Relationship between temperature and $\sqrt[3]{}$MI across the San Francisco Bay Area interacted with period of the week. (b) Relationship between temperature and mobility with each year modeled separately. Weekday and weekend relationships are plotted separately. (c) Relationship between temperature and $\sqrt[3]{}$MI on data that only includes hot days (See Section 2). (d) Relationship between temperature and mobility on hot days with each year modeled separately. Weekday and weekend relationships are plotted separately. For panels (a) and (c) median weekday response is indicated with a solid purple line, and weekend with a solid green line. For panels (b) and (d), relationship in 2020 shown in orange, and 2021 in purple. R^2 and projected (proj) r^2 values are reported for each model. Proj r^2 refers to the r^2 value of the estimated model without including fixed effects.
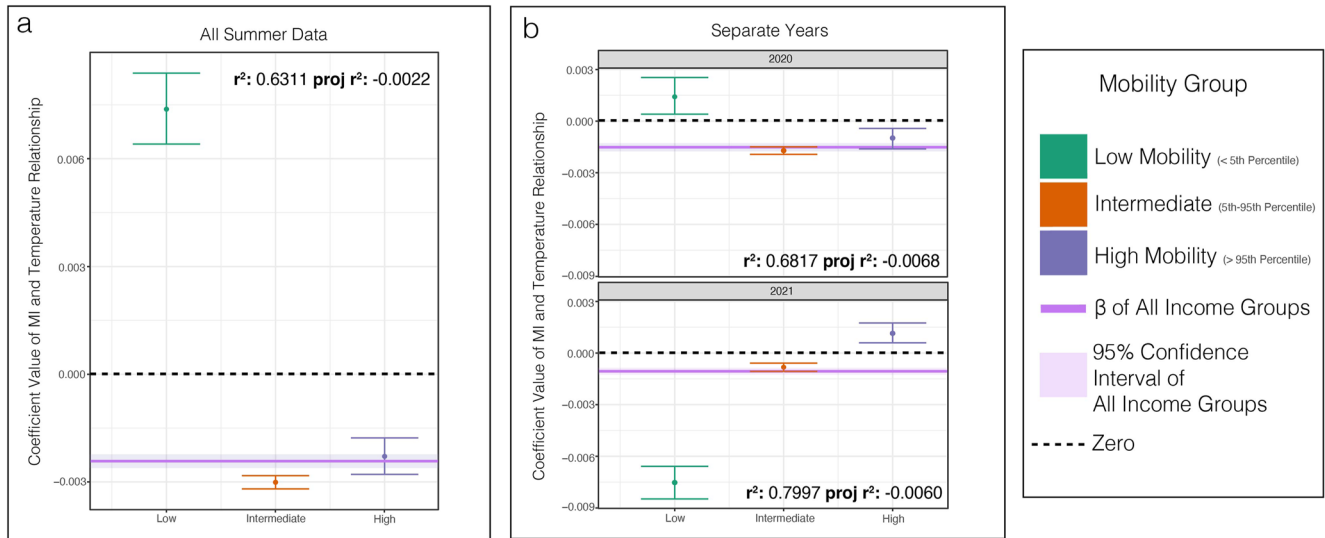
Figure 6. Resulting relationship between mobility index (MI) and temperature after the MI group interaction variable is integrated into the model. Points show median coefficient estimates and vertical bars show the 95% CI around each point estimate. Solid purple line and shaded area are model results from models in Figure 3a for comparison. Dotted black line indicates zero coefficient value.

with separate years (in particular with the "Low MI" group) are a result of differences in how week and month fixed effects were calculated in the two analyses. In the "all summer" model, the month and week fixed effects were included across both years, while the "separate year" models calculated the month and week fixed effects only in that year. Therefore more variation was removed by the fixed effects in the "separate year" models, resulting in a more conservative estimate. Note that due to size of the effect of temperature on mobility for the Low and High MI subgroups, values are not comparable to their log-transformations and should not be considered approximations of the percent change in MI with temperature (Table S2 in Supporting Information S1).

4. Discussion

Understanding mobility trends requires careful attention to the environment, as variation in time and space can lead to a wide range of relationships (Böcker et al., 2013). Hence, the mobility patterns uncovered by this study are specific only to the study period (2020 and 2021 summer) and location (SF Bay Area), and should be interpreted through a pandemic-era lens. However, when coupled with additional context and prior studies, there are several insights that can be gleaned from this analysis.

We are confident that our MI metric was able to capture variability in mobility through time within the region. There was a clear decline in mobility in the SF Bay Area following" the establishment of shelter in place policies in spring of 2020 (Figure 2a). For the 2 years we analyzed, average mobility increased steadily throughout 2021, coinciding with vaccine introductions and a general relaxation of shelter in place restrictions. Our analysis included periods of the pandemic with additional COVID-19 virus variants (Vasireddy et al., 2021) and a wide range of shelter in place policies that included multiple closures and re-openings (Eby, 2023). It also focused on a highly populated region that contains both metropolitan and rural areas, and high socio-demographic spatial heterogeneity. In addition to socioeconomic heterogeneity, the SF Bay Area also encompasses substantial climatic heterogeneity, including coastal and inland regions. The high variety of geographic features—including topography (mountains, inland valleys), and coastal exposure (Ekstrom & Moser, 2012)—contributes to the numerous distinct climatic zones. As expected, inland block groups have more days that reach extremely high temperatures than block groups closer to the Pacific coast or San Francisco Bay (Figure S4 in Supporting Information S1).

Given this, we believe that there is considerable value in investigating MI using the location-based fixed effects of our panel regression, which allowed us to better deduce and isolate the influence of temperature on mobility. Overall, our models consistently predicted that incremental increases in temperature resulted in decreased MI

during the study period. This result was nearly unanimous across all models (Figures 3–6) and would suggest some fraction of mobility behavior during the pandemic era was influenced by temperature. However, the rate of decrease in local, daily was impacted by multiple variables, including differences between hot days, weekends and weekdays, median income of destination, and the baseline level of mobility.

Weekdays were generally more resistant to reductions in mobility when compared to weekends (Figure 4), likely due to commute requirements. One potential interpretation of our results is that the weekend is more sensitive to any increase in temperature due to the split between typical weekend leisure travel and weekday work-commute travel. Although many individuals were able to shift to remote work, much of the population were "essential workers" and continued to commute to work (Borkowski et al., 2021; Qian et al., 2023). A number of studies have uncovered that commuter behavior tends to resist temperature-induced mobility changes when compared to leisure trips (Aaheim & Hauge, 2005; Cools et al., 2010; Sabir et al., 2011).

The response of mobility to temperature was also accentuated on hot days. For example, when we isolated the data set to only model days where at least 5% of block groups experienced extreme temperatures, we discovered that $\sqrt[3]{MI}$ decreased in response to increasing temperatures at a rate 2.5 times faster than on regular days (MI ~15 times faster) (Figure 3c). In addition, while there was typically a difference in weekend and weekday responses during the summer (Figures 4a and 4b), on hot days the rate of mobility reduction more than doubled compared to the full summer data set (Figure 3c), and the rate was the same for both periods of the week (Figures 4c and 4d). Our results thus suggest that periods of hot days are enough to overcome the weekday resistance to mobility changes due to temperature. Pandemic restrictions certainly reduced the number of individuals with required commutes (Borkowski et al., 2021; Qian et al., 2023), and potentially allowed for more flexibility in weather response during the weekdays. However, given that reductions in commute requirements were not universal (Newsom, 2020) and many essential workers were still required to work throughout the pandemic, there was potential for disparities in the ability to shelter on extremely hot days.

Throughout the 2-year period from 2020 to 2021, we found a link between our mobility metric and the median income of a block group (Figure 5). The fixed effects model with income interaction predicted a decrease in mobility in response to increasing temperature for all income groups. However, the highest earning block groups exhibited a more rapid decrease in $\sqrt[3]{MI}$ value in response to increasing temperatures. This means either that wealthier residents of these neighborhoods traveled in and out of their block group less frequently, and/or that fewer outside visitors entered these neighborhoods. Wealthy block groups exhibited a pattern of lower mobility that aligned with the intended effects of shelter in place policies (i.e., reduction or cessation of non-essential travel, shifting to remote work when possible, and limits on gatherings in an attempt to reduce virus transmission) (Newsom, 2020). Conversely, the Low income group had a significantly smaller rate of mobility reduction than the High income group (Figure 5). This aligns with prior studies that considered the impacts of COVID-19 policies on low-income individuals and found disparities in their ability to reduce daily travel (Chen et al., 2020; Dadashzadeh et al., 2022; Ruiz-Euler et al., 2020). For lower income groups, these results could potentially indicate fewer options to reduce mobility due to work or personal obligations. Lower income block groups showed a pattern of movement that was less aligned with the intended effects of shelter in place policies, with limited reductions when compared to other subsets of the population (Figure 5). Notably, any medically necessary travel was considered "essential" and therefore travel completed to reduce exposure to extreme heat and protect personal health was allowable under shelter in place (Newsom, 2020; SFDoH, 2020). However, such travel potentially required individuals to choose between continued heat exposure at home and the risk of exposure to COVID-19 outside the home. Since the median income value in our analysis was attributed to the visited block group, we cannot draw conclusions about the income status of those visiting the block groups. One possible interpretation is that as temperatures increased, areas that were wealthy (and thus more likely to have access to air conditioning or other heat abatement at home) could continue to comply with shelter in place orders.

It is important to emphasize that income alone cannot fully explain all the socio-demographic disparity in environmental (Banzhaf et al., 2019) and health (Zimmerman & Anderson, 2019) outcomes. The population of the SF Bay Area has variable sensitivities to extreme heat due to known risk factors such as prevalence of at-home cooling access (O'Neill et al., 2003), median age (Luber & McGeehin, 2008), racial background (Basu & Ostro, 2008), and ethnic background (Hansen et al., 2013). We stratified our data by income, which is known to itself influence health and wellbeing and is also correlated with other risk factors (Downey, 1998; Reid et al., 2009). However, while our study offers additional insight into mobility responses to temperature within a highly populated region

with severe income inequality, it does not offer a fully exhaustive directory of block groups most likely to see a more dramatic change in MI on a hot day. There are additional measures that may have had an influence on mobility that have yet to be tested, including air conditioning prevalence, race, and land use. However, data limitations make these analyses not feasible in the context of this study. More details on these limitations can be found in Supporting Information S1 (Text S3).

Finally, we investigated the mobility response of the most and least mobile block groups (based on their average summer MI) independently from the rest of the data set. We found that block groups with MI values that fell above the 95th percentile or below the 5th percentile often responded differently than the rest of the data (5th–95th percentile) and were sensitive to the differences between the 2 years studied (Figure 6). Areas with the lowest baseline mobility typically experienced increasing visits with increasing temperature in 2020, and those with the highest baseline mobility experienced decreases at a slower rate than the rest of the data set. In 2021, this relationship was reversed, and the least mobile locations saw the largest rate of decrease in MI of all models, while the highly mobile locations experienced increases in response to increasing temperature. This high sensitivity to year and temperature is yet another example of the significant variability in baseline mobility across the region, and the importance of context in understanding mobility trends. The distribution of average MI values were right skewed and there were many block groups with MI values that were an order of magnitude higher than the average (Figure S3 in Supporting Information S1). These locations represented areas that are highly trafficked, and often included points of interest (e.g., retail centers, tourist attractions, and downtown areas), and those that were least trafficked were often residential areas with few attractions (Table S5 in Supporting Information S1). Areas that enabled activities aligned with shelter in place guidelines were likely outdoors (e.g., parks, nature preserves), and thus could have been highly mobile in general but less appealing with hot temperatures. In 2021, a trend of reopenings and the availability of vaccines might have encouraged further travel into tourist locations or indoor air-conditioned spaces that may have had more limited availability during 2020.

5. Conclusions

We built upon prior studies of the relationship between heat and mobility using causal inference methods to explore how a unit change in temperature may change local, daily mobility. In particular, using panel regressions with fixed effects enabled us to control for unobserved variability between block groups and counties (e.g., common behavior patterns, infrastructure), and changes that occur over time that are common across the block groups or counties (e.g., federal, state, and municipal regulations). The results of the regression models with interaction variables allowed us to investigate how the period of the week, median income, and the most and the baseline mobility may influence the expected mobility in the summer, and during the hottest days of the year.

The patterns we uncovered add clarity to the previous understanding of the relationship between temperature and mobility (Badr et al., 2020; Böcker et al., 2016; Liu et al., 2014; Zhu et al., 2020) during a period when typical mobility patterns were already disrupted by COVID-19 policies. We show that during this pandemic period, increasing temperature generally resulted in decreased mobility, and the rate of decrease more than doubled when temperatures were extremely hot. Weekdays were generally more robust to changes than weekends. Our results also suggest that there is a fundamental difference in the temperature-mobility relationship between High and Low income block groups, with High income block groups further decreasing mobility in response to high temperatures, and Low income block groups decreasing at a slower rate (Figure 5). Thus, even in the presence of highly restrictive public health policies, high temperatures can lead to a range of mobility responses. Given the key role that local, daily mobility plays in public health interventions during periods of extreme heat, our results highlight a number of variables that influence that mobility in the SF Bay Area. These results are worthy of consideration for future mobility studies, transit planning, and heat mitigation efforts in highly populated regions, both in the current climate and in the future.

Conflict of Interest

The authors declare no conflicts of interest relevant to this study.

Data Availability Statement

The R scripts used to execute and report on the analyses in this paper can be found at https://github.com/aminaly/heatwave_covid, and is preserved on Zenodo at on Zenodo at https://zenodo.org/record/7434145. SafeGraph's raw mobility data can be accessed through registration on their website, https://www.safegraph.com/covid-19-da-

ta-consortium. gridMET data are available online for download at https://www.climatologylab.org/gridmet.html. American Community Survey Data can be accessed on the US Census Bureau's website, https://www.census.gov/programs-surveys/acs/data.html. Bay Area Air Quality Management District Data can be accessed through the website, https://www.baaqmd.gov/alertstatus.

References

Aaheim, H. A., & Hauge, K. E. (2005). Impacts of climate change on travel habits: A national assessment based on individual choices. Retrieved from https://pub.cicero.oslo.no/cicero-xmlui/handle/11250/191992

Abatzoglou, J. T. (2013). Development of gridded surface meteorological data for ecological applications and modeling. *International Journal of Climatology*, *33*(1), 121–131. https://doi.org/10.1002/joc.3413

American Housing Survey (AHS). (2018). American housing survey (AHS) [Dataset]. US Department of Housing and Urban Development. Retrieved from https://catalog.data.gov/dataset/american-housing-survey-ahs

Aragón, T. J. (2021). *"Travel advisory"*. Travel Advisory, California Department of Public Health. Retrieved from https://www.cdph.ca.gov/Programs/CID/DCDC/Pages/COVID-19/Travel-Advisory.aspx

Badr, H. S., Du, H., Marshall, M., Dong, E., Squire, M. M., & Gardner, L. M. (2020). Association between mobility patterns and COVID-19 transmission in the USA: A mathematical modelling study. *The Lancet Infectious Diseases*, *20*(11), 1247–1254. https://doi.org/10.1016/S1473-3099(20)30553-3

Banzhaf, H. S., Ma, L., & Timmins, C. (2019). Environmental justice: Establishing causal relationships. *Annual Review of Resource Economics*, *11*(1), 377–398. https://doi.org/10.1146/annurev-resource-100518-094131

Bassil, K. L., Cole, D. C., Moineddin, R., Craig, A. M., Wendy Lou, W. Y., Schwartz, B., & Rea, E. (2009). Temporal and spatial variation of heat-related illness using 911 medical dispatch data. *Environmental Research*, *109*(5), 600–606. https://doi.org/10.1016/j.envres.2009.03.011

Baston, D. (2022). exactextractr: Fast extraction from raster dataset using polygons. R package version 0.9.1 [Software]. CRAN.R. Retrieved from https://CRAN.R-project.org/package=exactextractr

Basu, R., & Ostro, B. D. (2008). A multicounty analysis identifying the populations vulnerable to mortality associated with high ambient temperature in California. *American Journal of Epidemiology*, *168*(6), 632–637. https://doi.org/10.1093/aje/kwn170

Batibeniz, F., Ashfaq, M., Diffenbaugh, N. S., Key, K., Evans, K. J., Turuncoglu, U. U., & Önol, B. (2020). Doubling of U.S. population exposure to climate extremes by 2050. *Earth's Future*, *8*(4), e2019EF001421. https://doi.org/10.1029/2019EF001421

Bay Area Air Quality Management District (BAAQMD). (2021). Spare the air every day. Retrieved from https://www.baaqmd.gov/alertstatus

Böcker, L., Dijst, M., & Faber, J. (2016). Weather, transport mode choices and emotional travel experiences. *Transportation Research Part A: Policy and Practice*, *94*, 360–373. https://doi.org/10.1016/j.tra.2016.09.021

Böcker, L., Dijst, M., & Prillwitz, J. (2013). Impact of everyday weather on individual daily travel behaviors in perspective: A literature review. *Transport Reviews*, *33*(1), 71–91. https://doi.org/10.1080/01441647.2012.747114

Borkowski, P., Jażdżewska-Gutta, M., & Szmelter-Jarosz, A. (2021). Lockdowned: Everyday mobility changes in response to COVID-19. *Journal of Transport Geography*, *90*, 102906. https://doi.org/10.1016/j.jtrangeo.2020.102906

Chen, K. L., Brozen, M., Rollman, J. E., Ward, T., Norris, K., Gregory, K. D., & Zimmerman, F. J. (2020). Transportation access to health care during the COVID-19 pandemic: Trends and implications for significant patient populations and health care needs. Retrieved from https://escholarship.org/uc/item/22b3b1rc

Collins, M., Knutti, R., Arblaster, J., Dufresne, J.-L., Fichefet, T., Gao, X., et al. (2013). Long-term climate change: Projections, commitments and irreversibility (Vol. *108*).

Cools, M., Moons, E., Creemers, L., & Wets, G. (2010). Changes in travel behavior in response to weather conditions: Do type of weather and trip purpose matter? *Transportation Research Record*, *2157*(1), 22–28. https://doi.org/10.3141/2157-03

Creemers, L., Wets, G., & Cools, M. (2015). Meteorological variation in daily travel behavior: Evidence from revealed preference data from The Netherlands. *Theoretical and Applied Climatology*, *120*(1), 183–194. https://doi.org/10.1007/s00704-014-1169-0

Dadashzadeh, N., Larimian, T., Levifve, U., & Marsetič, R. (2022). Travel behavior of vulnerable social groups: Pre, during, and post COVID-19 pandemic. *International Journal of Environmental Research and Public Health*, *19*(16), 10065. https://doi.org/10.3390/ijerph191610065

Diffenbaugh, N. S., & Ashfaq, M. (2010). Intensification of hot extremes in the United States. *Geophysical Research Letters*, *37*(15), L15701. https://doi.org/10.1029/2010GL043888

Diffenbaugh, N. S., Field, C. B., Appel, E. A., Azevedo, I. L., Baldocchi, D. D., Burke, M., et al. (2020). The COVID-19 lockdowns: A window into the Earth system. *Nature Reviews Earth & Environment*, *1*(9), 470–481. https://doi.org/10.1038/s43017-020-0079-1

Diffenbaugh, N. S., Singh, D., & Mankin, J. S. (2018). Unprecedented climate events: Historical changes, aspirational targets, and national commitments. *Science Advances*, *4*(2), eaao3354. https://doi.org/10.1126/sciadv.aao3354

Downey, L. (1998). Environmental injustice: Is race or income a better predictor? *Social Science Quarterly*, *79*(4), 766–778. Retrieved from https://www.jstor.org/stable/42863846

Eby, K. (2023). Coronavirus timeline: Tracking major moments of COVID-19 pandemic in San Francisco Bay area. Retrieved from https://abc7news.com/timeline-of-coronavirus-us-covid-19-bay-area-sf/6047519/

Eisenman, D. P., Wilhalme, H., Tseng, C.-H., Chester, M., English, P., Pincetl, S., et al. (2016). Heat death associations with the built environment, social vulnerability and their interactions with rising temperature. *Health & Place*, *41*, 89–99. https://doi.org/10.1016/j.healthplace.2016.08.007

Ekstrom, J. A., & Moser, S. C. (2012). Climate change impacts, vulnerabilities, and adaptation in the San Francisco Bay area: A synthesis of PIER program reports and other relevant research. Retrieved from https://escholarship.org/uc/item/9qx629fh

Gronlund, C. J., & Berrocal, V. J. (2020). Modeling and comparing central and room air conditioning ownership and cold-season in-home thermal comfort using the American Housing Survey. *Journal of Exposure Science and Environmental Epidemiology*, *30*(5), 814–823. https://doi.org/10.1038/s41370-020-0220-8

Hansen, A., Bi, L., Saniotis, A., & Nitschke, M. (2013). Vulnerability to extreme heat and climate change: Is ethnicity a factor? *Global Health Action*, *6*(1), 21364. https://doi.org/10.3402/gha.v6i0.21364

Head, J. R., Andrejko, K. L., Cheng, Q., Collender, P. A., Phillips, S., Boser, A., et al. (2020). The effect of school closures and reopening strategies on COVID-19 infection dynamics in the San Francisco Bay area: A cross-sectional survey and modeling analysis. *medRxiv*. https://doi.org/10.1101/2020.08.06.20169797

Hobbs, R. J., Richardson, D. M., & Davis, G. W. (1995). Mediterranean-type ecosystems: Opportunities and constraints for studying the function of biodiversity. In G. W. Davis, & D. M. Richardson (Eds.), *Mediterranean-type ecosystems* (Vol. 109, pp. 1–42). Springer Berlin Heidelberg. https://doi.org/10.1007/978-3-642-78881-9_1

IPCC. (2021). Climate change 2021: The physical science basis. In V. Masson-Delmotte, P. Zhai, A. Pirani, S. L. Connors, C. Péan, et al. (Eds.), *Contribution of working group I to the sixth assessment report of the intergovernmental panel on climate change*. Cambridge University Press. In press. https://doi.org/10.1017/9781009157896

Jung, Y. (2021). The Bay Area is getting hotter. Is air conditioning becoming standard for homes here? Retrieved from https://www.sfchronicle.com/local/article/How-many-Bay-Area-homes-have-air-conditioning-16273057.php

Liu, C., Susilo, Y. O., & Karlström, A. (2014). Examining the impact of weather variability on non-commuters' daily activity–travel patterns in different regions of Sweden. *Journal of Transport Geography*, *39*, 36–48. https://doi.org/10.1016/j.jtrangeo.2014.06.019

Luber, G., & McGeehin, M. (2008). Climate change and extreme heat events. *American Journal of Preventive Medicine*, *35*(5), 429–435. https://doi.org/10.1016/j.amepre.2008.08.021

Newsom, G. (2020). Executive order. No. N-33-20 (p. 2).

O'Neill, M. S., Zanobetti, A., & Schwartz, J. (2003). Modifiers of the temperature and mortality association in seven US cities. *American Journal of Epidemiology*, *157*(12), 1074–1082. https://doi.org/10.1093/aje/kwg096

O'Neill, M. S., Zanobetti, A., & Schwartz, J. D. (2005). Disparities by race in heat-related mortality in four US cities: The role of air conditioning prevalence. *Journal of Urban Health: Bulletin of the New York Academy of Medicine*, *82*(2), 191–197. https://doi.org/10.1093/jurban/jti043

Palecki, M. A., Changnon, S. A., & Kunkel, K. E. (2001). The nature and impacts of the July 1999 heat wave in the Midwestern United States: Learning from the Lessons of 1995. *Bulletin of the American Meteorological Society*, *82*(7), 1353–1368. https://doi.org/10.1175/1520-0477(2001)082<1353:TNAIOT>2.3.CO;2

Pucher, J., & Buehler, R. (2012). *City cycling*. MIT Press.

Qian, X., Jaller, M., & Circella, G. (2023). Exploring the potential role of bikeshare to complement public transit: The case of San Francisco amid the coronavirus crisis. *Cities*, *137*, 104290. https://doi.org/10.1016/j.cities.2023.104290

Reid, C. E., O'Neill Marie, S., Gronlund, C. J., Brines, S. J., Brown, D. G., Diez, -R. A. V., & Schwartz, J. (2009). Mapping community determinants of heat vulnerability. *Environmental Health Perspectives*, *117*(11), 1730–1736. https://doi.org/10.1289/ehp.0900683

Reidmiller, D. R., Avery, C. W., Easterling, D. R., Kunkel, K. E., Lewis, K. L. M., Maycock, T. K., & Stewart, B. C. (2018). Impacts, risks, and adaptation in the United States: The fourth national climate assessment, volume II. *U.S. Global Change Research Program*, https://doi.org/10.7930/NCA4.2018

Ruiz-Euler, A., Privitera, F., Giuffrida, D., Lake, B., & Zara, I. (2020). Mobility patterns and income distribution in times of crisis: U.S. Urban centers during the COVID-19 pandemic. In *SSRN scholarly paper*. https://doi.org/10.2139/ssrn.3572324

Sabir, M., Van Ommeren, J., Koetse, M., & Rietveld, P. (2011). Adverse weather and commuting speed. *Networks and Spatial Economics*, *11*(4), 701–712. https://doi.org/10.1007/s11067-010-9130-y

SafeGraph (2022). SafeGraph COVID-19 data consortium [Dataset]. https://www.safegraph.com/covid-19-data-consortium

San Francisco Department of Health (SFDoH). (2020). Health officer. *Order of the Health Officer No. C19-07 (Shelter in Place)*, *16*. Retrieved from https://sfgsa.org/sites/default/files/Document/OrderC19-07ShelterinPlace.pdf

Studdert, D. M., Hall, M. A., & Mello, M. M. (2020). Partitioning the curve—Interstate travel restrictions during the Covid-19 pandemic. *New England Journal of Medicine*, *383*(13), e83. https://doi.org/10.1056/NEJMp2024274

UNWTO. (2020). 100% of global destinations now have COVID-19 travel restrictions, UNWTO reports|UNWTO. Retrieved from https://www.unwto.org/news/covid-19-travel-restrictions

US Census Bureau. (2022). 2015-2019 American community survey data [Dataset]. Census. Retrieved from https://www.census.gov/programs-surveys/acs/data.html

Vant-Hull, B., Ramamurthy, P., Havlik, B., Jusino, C., Corbin-Mark, C., Schuerman, M., et al. (2018). The Harlem heat project: A unique media–community collaboration to study indoor heat waves. *Bulletin of the American Meteorological Society*, *99*(12), 2491–2506. https://doi.org/10.1175/BAMS-D-16-0280.1

Vasireddy, D., Vanaparthy, R., Mohan, G., Malayala, S. V., & Atluri, P. (2021). Review of COVID-19 variants and COVID-19 vaccine efficacy: What the clinician should know? *Journal of Clinical Medicine Research*, *13*(6), 317–325. https://doi.org/10.14740/jocmr4518

WHO Director-General's opening remarks at the media briefing on COVID-19-11 March 2020. (2020). WHO Director-General's opening remarks at the media briefing on COVID-19-11 March 2020. Retrieved from https://www.who.int/director-general/speeches/detail/who-director-general-s-opening-remarks-at-the-media-briefing-on-covid-19---11-march-2020

Widerynski, S., Schramm, P., Conlon, K., Noe, R., Grossman, E., Hawkins, M., et al. (2017). The use of cooling centers to prevent heat-related illness: Summary of evidence and strategies for implementation (Climate and Health Technical Report Series). *Climate and Health Program, Centers for Disease Control and Prevention*. https://stacks.cdc.gov/view/cdc/47657

Wu, Y., Mooring, T. A., & Linz, M. (2021). Policy and weather influences on mobility during the early US COVID-19 pandemic. *Proceedings of the National Academy of Sciences of the United States of America*, *118*(22), e2018185118. https://doi.org/10.1073/pnas.2018185118

Zacharias, J., Stathopoulos, T., & Wu, H. (2004). Spatial behavior in San Francisco's plazas: The effects of microclimate, other people, and environmental design. *Environment and Behavior*, *36*(5), 638–658. https://doi.org/10.1177/0013916503262545

Zhu, L., Liu, X., Huang, H., Avellán-Llaguno, R. D., Lazo, M. M. L., Gaggero, A., et al. (2020). Meteorological impact on the COVID-19 pandemic: A study across eight severely affected regions in South America. *Science of the Total Environment*, *744*, 140881. https://doi.org/10.1016/j.scitotenv.2020.140881

Zimmerman, F. J., & Anderson, N. W. (2019). Trends in health equity in the United States by race/ethnicity, sex, and income, 1993-2017. *JAMA Network Open*, *2*(6), e196386. https://doi.org/10.1001/jamanetworkopen.2019.6386

References From the Supporting Information

Ahn, Y., & Uejio, C. K. (2022). Modeling air conditioning ownership and availability. *Urban Climate*, *46*, 101322. https://doi.org/10.1016/j.uclim.2022.101322

Menendian, S., Gambhir, S., French, K., & Gailes, A. (2023). *Single-family zoning in the San Francisco Bay area: Characteristics of exclusionary communities*. Othering & Belonging Institute.